

# RSC Advances



This is an *Accepted Manuscript*, which has been through the Royal Society of Chemistry peer review process and has been accepted for publication.

*Accepted Manuscripts* are published online shortly after acceptance, before technical editing, formatting and proof reading. Using this free service, authors can make their results available to the community, in citable form, before we publish the edited article. This *Accepted Manuscript* will be replaced by the edited, formatted and paginated article as soon as this is available.

You can find more information about *Accepted Manuscripts* in the [Information for Authors](#).

Please note that technical editing may introduce minor changes to the text and/or graphics, which may alter content. The journal's standard [Terms & Conditions](#) and the [Ethical guidelines](#) still apply. In no event shall the Royal Society of Chemistry be held responsible for any errors or omissions in this *Accepted Manuscript* or any consequences arising from the use of any information it contains.

## ARTICLE

# Revisiting the principles of preparing aqueous quantum dots for biological applications: the effects of surface ligands on the physicochemical property of quantum dots

Cite this: DOI: 10.1039/x0xx00000x

Received xxxx,  
Accepted xxxx

DOI: 10.1039/x0xx00000x

[www.rsc.org/](http://www.rsc.org/)

Butian Zhang,<sup>a</sup> Rui Hu,<sup>a</sup> Yucheng Wang,<sup>a</sup> Chengbin Yang,<sup>a</sup> Xin Liu<sup>b</sup> and Ken-Tye Yong<sup>\*,a</sup>

Surface functionalization of quantum dots (QDs) is one of the most important aspects for the designing and preparing the desired QDs for specific biomedical applications. The surface ligands not only render the QDs water-dispersible, but also endow them with different functional groups for bioconjugation. More importantly, as the surface ligand layer on QD surface is responsible in interacting with the biological environments, the type of surface ligands will greatly affect the response from the cells, such as the cellular uptake and cytotoxicity. In this paper, we investigate the effects of surface ligand on the physicochemical properties of QDs and examine different QD formulations for possible biomedical applications. Seven types of QD formulations were prepared by anchoring the CdSe/CdS/ZnS QDs surface with either short-chain mercapto ligands (MPA, MSA, cysteine, AET) or PEG derivative ligands (mPEG-SH, CM-PEG-SH, NH<sub>2</sub>-PEG-SH). We then conducted a systematic study to evaluate the colloidal stability, photostability, cellular uptake and *in vitro* toxicity of the formulations. The colloidal stability was evaluated by the particle size change in water, acidic/neutral/alkaline buffer solutions and cell culture medium. Our results show that the carboxyl-terminated QDs have the best colloidal stability in water and alkaline solutions. PEG-capped QDs are more stable than short-chain ligand modified QDs in cell culture medium. For the photostability of different QD formulations under UV irradiation, we observed that the MPA-, MSA- and Cys-QDs had better photostability than that of the PEG modified QDs, whereas the AET-QD is the least stable one. Cellular uptake of QDs was evaluated using cell imaging and quantified by flow cytometry. The PEG chains and surface charge of QDs were found to play critical roles in the cellular uptake. Using RAW246.7 macrophage cells as the cellular uptake model, we discovered that the anionic QDs had a much higher uptake compared to the cationic QD formulations. In general, each set of prepared QD formulation with specific type of surface ligands display certain strengths and limitations in different aspects of their physicochemical properties. Therefore, one should carefully consider and choose the type of QD formulation in the experiments thereby minimizing its impacts arising from their limitations.

## Introduction

For the last decade, quantum dots (QDs) have shown great potential in biomedical applications.<sup>1-7</sup> In comparison to conventional organic dyes, they possess comparable quantum yield (QY), excellent photostability, broad absorption spectra, narrow photoluminescence (PL) spectra and long fluorescence lifetime.<sup>8-10</sup> Moreover, their emission peak is size- and shape-dependent thereby allowing one to use them for multiplex fluorescence imaging *in vitro* and *in vivo*.<sup>11, 12</sup> These unique optical properties have made QDs promising probes for applications ranging from sensing to medicine.<sup>7, 13-15</sup> However, there remains a significant challenge to preserve the optical property of water-dispersible QD formulations with long shelf lives. Currently, many of the QD formulations are known to have short shelf lives from few hours to few days.<sup>3, 16-18</sup> As time progresses, some precipitation or aggregation of QDs will take place in aqueous phase or biological buffers. Such phenomena will adversely impact the optical property of QDs and may lead

to skewing of data analysis when different quality of QDs is used in the experiments. Thus, there is an urgent need to further investigate and understand the root cause of the degradation of the optical property of QDs in biological mediums. In general, QDs are commonly synthesized in a reaction mixture containing organic solvents and surfactants.<sup>19, 20</sup> As such, the QDs prepared in this method are capped with hydrophobic ligands on their surface and they do not readily disperse in aqueous phase and further surface modification steps are needed to make them water dispersible for biological applications.<sup>21-23</sup> These surface modification steps not only made QDs with water dispersible, but they also allow one to insert additional functionalities to the QDs formulations such as conjugating of biomolecules for targeting delivery and functionalization of MRI contrast agents for multimodal imaging.<sup>24, 25</sup> Thus, it is crucial for one to carefully design and optimize the surface modification steps for creating long shelf life of water dispersible QDs with comparable optical property as they are dispersed in organic phase for biomedical use.

There are two approaches that have been commonly used for making water dispersible QDs. The first approach involves encapsulating QDs surface with biocompatible materials such as amphiphilic polymers<sup>26</sup> and inorganic shells.<sup>27, 28</sup> This method offers the advantage of protecting the QD core from degradation in the biological environment. It is worth noting that this method will cause the overall QDs size to increase and may impact the intracellular mobility of the QDs if additional surface modification steps are not applied.<sup>3, 29</sup> The second method involves ligand exchange process. In the ligand exchange process, hydrophobic surfactants-functionalized QDs dispersion is mixed with excessive amount of heterobifunctional surfactants such as mercaptoacetic acid, mercaptosuccinic acid, mercaptopropionic acid, aminoethanethiol, allowing functional groups (e.g. thiol or amine group) attaching on the QD surface, and the other functional groups (e.g. carboxyl or amino group) extending out from the QDs surface to favorably interact with water.<sup>30-32</sup> During the ligand exchange process, the hydrophobic moieties attached to the QD surface are displaced by the heterobifunctional surfactants through a mass driven process and the bifunctional ligands depositing to the QD surface will provide them with water dispersibility. In some occasions, monofunctional surfactants (e.g. thiolated PEG molecules and amino PEG molecules) are used to functionalize the QDs surface for specific applications such as long term *in vivo* imaging. The variation of ligands used in functionalizing the QDs surface will greatly influence the physical, colloidal and optical property of the QDs formulation. For instance, the overall QDs hydrodynamic size is mainly determined by the structure and length of the ligands use during the ligand exchange process.<sup>33</sup> The surface charge density of QDs is affected by the functional groups and the grafting density of the ligands anchored on the QDs surface.<sup>34</sup> The colloidal stability of the QDs is governed by the polarity of functional groups present in the ligands. Generally, solubility is controlled by intermolecular forces at the molecular level and the polarity level of the molecules plays an important role for dissolving in polar solvents such as water and alcohols. This is why QDs functionalized with less polar ligands like mercaptoundecanoic acid or mercaptohexadecanoic acid do not disperse well in water but they do disperse to a good extent in most organic solvents.<sup>35</sup> Also, it is reported that the degradation of QDs is effected by the types of surface ligands functionalized on their surface.<sup>36</sup> In this work, we perform a comprehensive study on investigating the effects of surface ligands on the overall physical, colloidal and optical property of QDs and systematically evaluating the suitability of each type of ligand-functionalized QDs formulations for biological applications. Specifically, seven common types of surface ligands with different structures, lengths and functional groups (mercaptoacetic acid, mercaptosuccinic acid, cysteine, aminoethanethiol, methoxy-PEG-Thiol, carboxymethyl-PEG-thiol and amine-PEG-thiol molecules) were chosen to prepare water dispersible CdSe/CdS/ZnS QDs where these QDs were originally capped with hydrophobic surfactants such as trioctylphosphine (TOP) and trioctylphosphine oxide (TOPO). The colloidal stability, photostability, cellular uptake and cytotoxicity of the prepared QD formulations were systematically studied and compared. Some important guidelines are highlighted to prepare the best quality of QDs aqueous dispersion for imaging applications. Our study has provided useful information on understanding the impacts of

surface ligands in designing specific type of QDs for different intended biomedical use.

## Materials and Experimental Methods

### Materials

3-mercaptopropionic acid (MPA), mercaptosuccinic acid (MSA), DL-Cysteine (Cys, 97%), cysteamine hydrochloride (2-Aminoethanethiol hydrochloride, AET•HCl,  $\geq 98\%$ ), chloroform, methanol and ammonium hydroxide solution ( $\text{NH}_4\text{OH}$ , 28.0%-30.0%  $\text{NH}_3$  basis) were purchased from Sigma-Aldrich. Methoxy-PEG-Thiol (mPEG-SH, Mw 5000), Carboxymethyl-PEG-Thiol (CM-PEG-SH, Mw 5000) and Amine-PEG-Thiol ( $\text{NH}_2$ -PEG-SH, Mw 5000) were obtained from Laysan Bio Inc. n-Hexane (95%) was purchased from Tedia. CertiPUR Buffer Solutions (pH 4.00/7.00/10.00, 20 °C) were products of Merck. Phosphate buffered saline (PBS) 7.2 was purchased from Gibco. Milli-Q 18.2  $\text{M}\Omega\cdot\text{cm}$  deionized (DI) water was used through the experiment. All chemicals were used as received without further purification. CdSe/CdS/ZnS QDs coated with TOP/TOPO were prepared using hot colloidal synthesis method and they were dissolved in chloroform and washed with ethanol before use.

### Preparing water-dispersible QDs using ligand exchange process

To prepare water-dispersible QDs, seven kinds of thiolated ligand molecules were used for the QDs phase transfer process. The typical methods for the QDs phase transfer process are replacing the TOP/TOPO capping layer on QDs by short-chain mercapto ligands (e.g. MPA, MSA, Cys and AET) and thiolated PEG derivatives (e.g. mPEG-SH, CM-PEG-SH and  $\text{NH}_2$ -PEG-SH). In our study, we have optimized the reaction parameters in the phase transfer process for obtaining water-dispersible QDs with the highest quality of enhanced PL intensity and biocompatibility. In the case of modifying the QDs surface with short-chain thiol ligands, MPA (4  $\mu\text{l}$ ) or MSA (33 mg) dissolved in 1 ml of chloroform or Cys (2 mg) dissolved in 1 ml of methanol was mixed with 1 mg of TOP/TOPO-capped CdSe/CdS/ZnS QDs dispersed in 5 ml of chloroform and the mixture were stirred for 5 min. After 5 min, 1 ml of  $\text{NH}_4\text{OH}$  solution with optimal concentration (3% for MPA, MSA and 20% for Cys respectively) was added into the reaction mixture and the biphasic solution system was continued to stir for another 5 h. After the stirring, majority of QDs were transferred to aqueous phase and they were then collected and washed by centrifugation with ethanol, and subsequently redispersed and stocked in 1 ml of DI water. To modify the QDs surface with AET surfactants, 100  $\mu\text{l}$  of AET•HCl solution in methanol (5  $\text{mg ml}^{-1}$ ) was added dropwise into 5 ml of QDs chloroform solution (0.2  $\text{mg ml}^{-1}$ ), followed by vigorous stirring. At this stage, flocculation was formed in the system and the system was then dissolved by DI water with gentle shaking. After 10 min centrifugation (6000 rpm) to remove agglomerates, the AET capped QDs was collected by 100-kDa filter with centrifugation and redispersed in DI water for future use. To prepare PEGylated QDs, mPEG-SH (8 mg), CM-PEG-SH (5 mg) or  $\text{NH}_2$ -PEG-SH (10 mg) dissolved in 2 ml of chloroform was mixed with 100  $\mu\text{l}$  of QD chloroform solution (10  $\text{mg ml}^{-1}$ ) and the mixture was stirred overnight. The QDs were then collected by adding hexane to the mixture. Before dispersing QDs to the aqueous phase, they were washed with the mixture of ethanol and hexane (v/v ratio 3:5) and centrifuged at a speed of 6000 rpm for 10 min.

### QDs Characterization

Fourier transform infrared (FT-IR) spectra were measured by a Shimadzu FT-IR spectrometer. Transmission electron microscopy (TEM) images were obtained using a JEOL JEM 2010 microscope. UV-vis absorption spectra of QDs dispersion were recorded using a Shimadzu UV-2450 spectrometer. The photoluminescence emission spectra of QDs dispersion were collected on a Fluorolog-3 Fluorometer (HORIBA Jobin Yvon, Edison, NJ USA). Zeta potential of the prepared QDs formulations was obtained by a ZetaPALS zeta potential analyzer (Brookhaven Instruments, NY USA). The QDs photostability study was performed by using G10T8 UV lamp (Watts: 10W, Spectral Output: 254nm) for irradiation.

### Investigating the stability of QDs in water, buffer solutions and DMEM medium

To evaluate the colloidal stability of the prepared QD formulations, the hydrodynamic diameters of the prepared QDs dispersed in DI water, CertiPUR Buffer Solutions (pH = 4.00, 7.00 and 10.00, at 20°C) and Dulbecco's Modified Eagle's Medium (DMEM, Gibco) were monitored by using dynamic light scattering (DLS) technique. A 90Plus particle size analyzer (Brookhaven Instruments, NY USA) was used in this study.

### Cell uptake of QDs study

RAW246.7 macrophage cells were cultured in DMEM supplemented with 10% fetal bovine serum (FBS, Hyclone), penicillin (100  $\mu\text{g ml}^{-1}$ , Gibco) and streptomycin (100  $\mu\text{g ml}^{-1}$ , Gibco) in a humidified environment (37 °C, 5%  $\text{CO}_2$ ). Before treating the cells with QDs, cells were seeded onto cover glasses in a 12-well plate with DMEM medium. The prepared QD formulations were then diluted to the same PL intensity for cellular uptake study. Next, the cells were treated with different QD formulations for 4 h. After 4 h of incubation, the treated cells were washed with PBS buffer for three times and fixed using 4% of formaldehyde solution. The nuclei were stained with 4',6-Diamidino-2-phenylindole dihydrochloride (DAPI, Sigma) for imaging analysis. Nikon Eclipse Ti inverted Microscope with a 60x oil-immersion lens was used for cell imaging study. Flow cytometry study was performed using a FACSCalibur flow cytometer system (Becton Dickinson, Mississauga, CA).

### Cell viability study

Cell viability was performed by using the MTT (3-(4,5-dimethylthiazol-2-yl)-2,5-diphenyltetrazolium bromide, Sigma) assay. Cells seeded in 96-well plates were incubated with QD formulations with different concentrations (sample wells) or same amount of PBS (control wells) for 24 h. It should be noted that the concentrations of the different QD formulations were determined based on the mass of the TOP/TOPO QDs before ligand exchange. After that, 18  $\mu\text{l}$  of MTT (5  $\text{mg ml}^{-1}$ ) solution was added to each well and the cells were incubated for another 4 h at 37 °C with 5%  $\text{CO}_2$ . Then the solution in the wells was decanted and the purple precipitate was solubilized by adding 150  $\mu\text{L}$  of dimethyl sulfoxide (DMSO, Sigma) to the sample wells. The absorbance of the solution in the sample wells was measured with a microplate reader (Bio-Rad) at a wavelength of 490 nm. The cell viability was obtained by normalizing the absorbance of the sample wells against that of the control wells.

### SiRNA Delivery by AET capped QDs

SiRNA<sup>FAM</sup> was mixed with different amount of AET-QDs formulations. After 20 min incubation at room temperature, the mixtures were loaded on a 1.2% agarose gel and electrophoresed at 100 V for 15 min. RAW246.7 macrophages were incubated with the QD-siRNA<sup>FAM</sup> complexes for 3 h, after that fluorescent imaging was taken.

### Results and Discussion

In this work, we have prepared CdSe/CdS/ZnS QDs based on our previous reported method.<sup>37</sup> The synthesized QDs are dispersed in organic solvent and capped by TOP/TOPO surfactants. Seven different surfactants, namely, MPA (mercaptopropionic acid), MSA (mercaptosuccinic acid), Cys (DL-Cysteine), AET (2-Aminoethanethiol hydrochloride), mPEG (Methoxy-PEG-Thiol), CM-PEG (Carboxymethyl-PEG-Thiol) and  $\text{NH}_2$ -PEG (Amine-PEG-Thiol) were used for preparing water dispersible QDs surface via ligand exchange process. FT-IR spectroscopy was firstly used to examine the exchange of the capping ligands on QDs. Figure 1 shows the representative FT-IR spectra of MSA, mPEG and TOP/TOPO capped QDs. The broad bands around 3000-3600  $\text{cm}^{-1}$  for all the samples may arise from the hydroxyl groups and  $\text{H}_2\text{O}$  bound on the QDs surface.<sup>38, 39</sup> The characteristic bands of S-H stretch at 2565  $\text{cm}^{-1}$  are present in MSA molecules. Figure 1a shows that the S-H stretch band disappeared after the ligand exchange process, which indicates the successful bonding between the sulfur atom and the QD surface.<sup>40, 41</sup> Also, the broad P=O bands around 1074  $\text{cm}^{-1}$ <sup>42, 43</sup> for TOP/TOPO capped QDs almost disappeared after MSA bonding. These changes suggest that the original TOP/TOPO on QDs surface is effectively replaced by MSA ligands. For ligand exchange with mPEG, strong peak of -CH stretch at 2886  $\text{cm}^{-1}$ , C-O-C stretch at 1114  $\text{cm}^{-1}$ <sup>44</sup> and other characteristic bands of mPEG<sup>45</sup> are observed in mPEG capped QDs, indicating the coating of mPEG on QD surface (Figure 1b). However, as these characteristic bands overlap with the -CH vibrations and P=O stretch, we were not able to determine whether the TOPO are completely removed. Figure 2a shows the absorption and photoluminescence (PL) spectra of the hydrophobic moieties-functionalized QDs and various surface ligands-modified QD formulations. Upon comparing to the TOP/TOPO-coated QDs chloroform dispersion, no significant changes were observed for the absorption and PL spectra of the prepared water-dispersible QD formulations. Figure 2b shows the TEM image of the QDs capped with TOP/TOPO surfactants. The high resolution image shows that the QDs are highly crystalline and have an average diameter of 6 nm. After ligand exchange process, the hydrodynamic sizes of the QDs were measured using DLS technique. The result shows that AET-QDs (~25nm) display a larger hydrodynamic diameter than that of MPA-, MSA- and Cys-QDs (7-10nm). From the TEM images, we can also observe some agglomerates after modifying the QDs surface with AET (Figure 2c). This is probably because the QD formulations may form different extents of ionic combinations and similar observations have been reported by Hoshino et al.<sup>36</sup> Figure 3 shows the zeta potential values for all the prepared surface modified QD formulations. QDs modified with surfactants containing carboxyl group show negatively charged surface and the QDs functionalized with surfactant containing amino group are determined to be positively charged. It should be noted that, for Cys-capped QDs, the negative zeta potential value could be attributed to the domination of the carboxyl

group dissociation rather than the amino group protonation under the pH of DI water (the isoelectric point of cysteine is  $\text{pH} = 5.02$ ). In addition, we have observed that surface ligand possesses with only carboxyl or amino groups (e.g. MPA, MSA, AET) will result in a much higher absolute zeta potential values upon comparing them to long-chain ligands (CM-PEG,  $\text{NH}_2$ -PEG). This could be resulted either from the higher ligand packing density or the smaller size of ligands that are capped on the QDs surface.<sup>29</sup> The different ligand dimensions may cause a wide diversity in ligand packing density. In this paper, we employed a geometric model to calculate the ligand packing

density by assuming the spherical nanocrystals and cone-shaped ligands (Figure S1).<sup>46, 47</sup> Based on the ligand dimensions from previous experimental results,<sup>48, 49, 50</sup> we estimated that the maximum possible packing density is  $\sim 4524$  per QD for short chain ligands and  $\sim 355$  per QD for PEG ligands. Considering the details such as the incomplete exchange of TOP/TOPO<sup>51</sup> and the repulsive force between molecules, the real situation could be more complicated. Nevertheless, this estimation still reveals the significant difference of the packing density between the short chain and PEG long chain ligands.

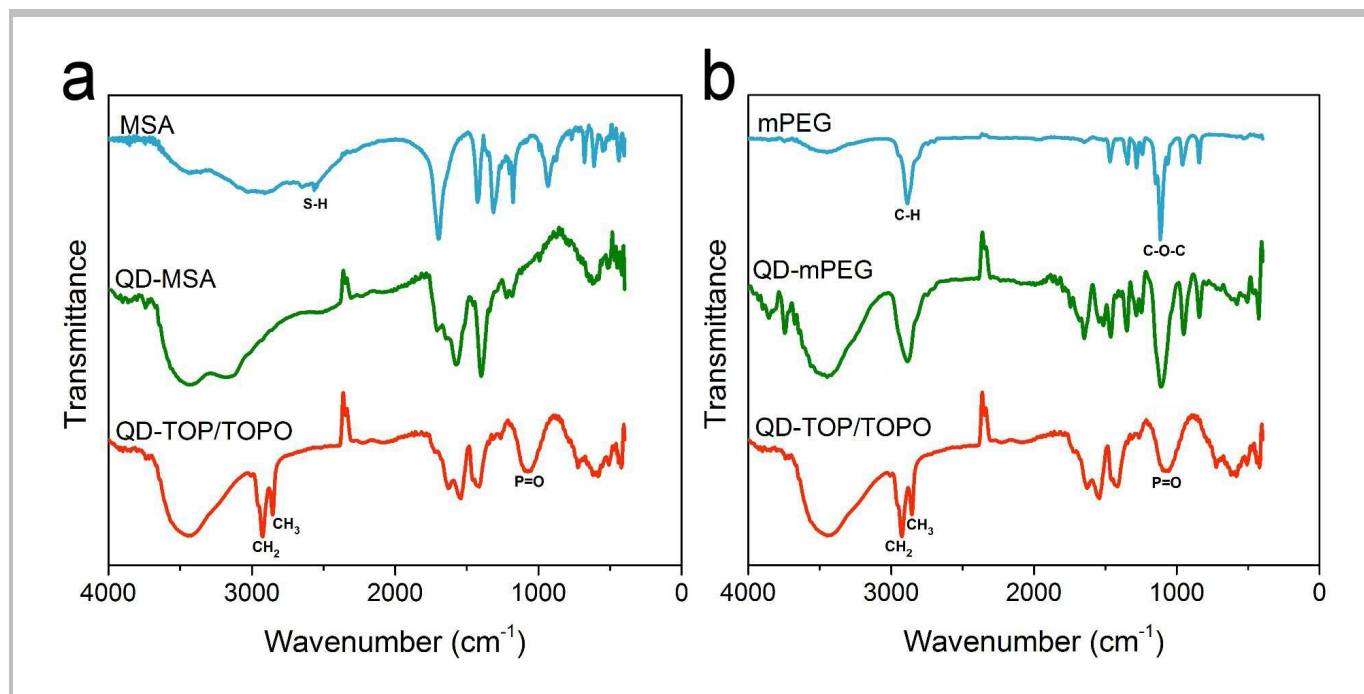


Figure 1. (a) FT-IR spectra of MSA, MSA capped QDs and TOP/TOPO capped QDs. (b) FT-IR spectra of mPEG, mPEG capped QDs and TOP/TOPO capped QDs.

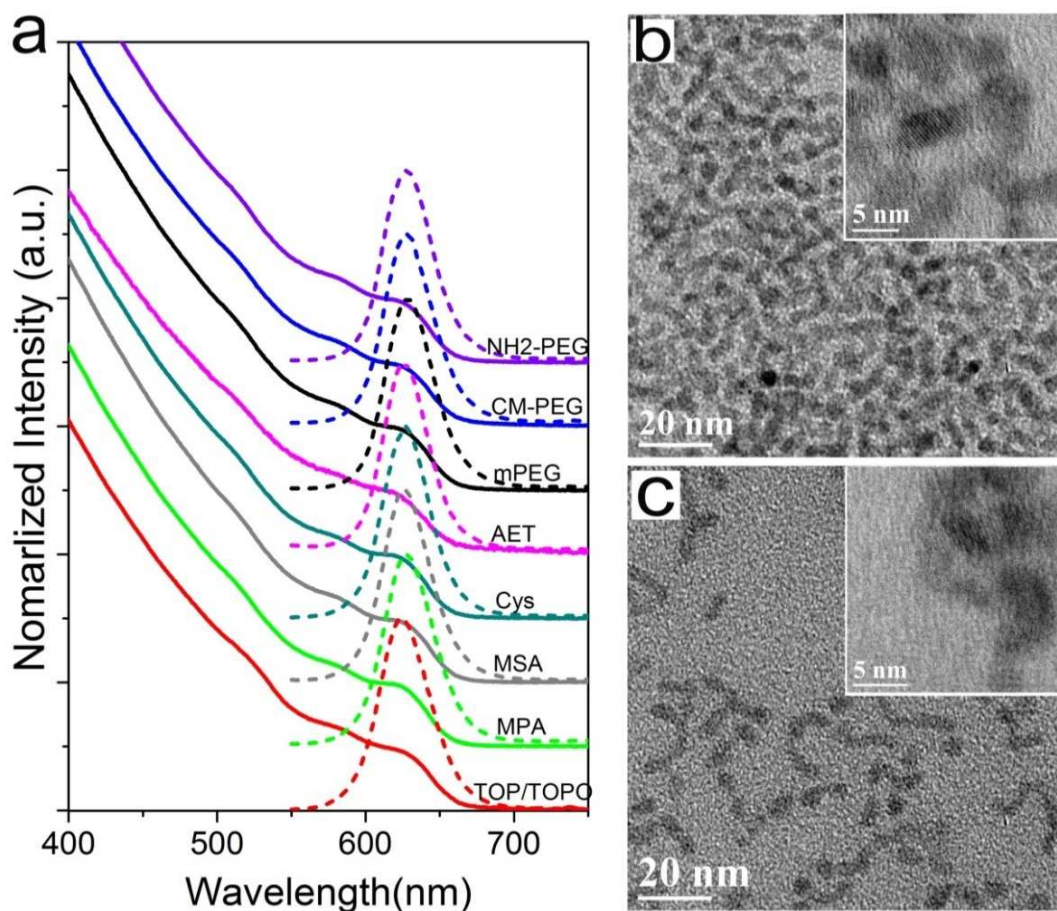


Figure 2. Characterization of QDs before and after ligand exchange. (a) Absorption (solid) and photoluminescence spectra (dashed) of CdSe/CdS/ZnS QDs before ligand exchange capped with TOP/TOPO (in chloroform) and after ligand exchange capped with different surfactants: MPA, MSA, Cys, AET, mPEG, CM-PEG, NH<sub>2</sub>-PEG (in water). (b) and (c) are TEM images of TOP/TOPO QDs and AET-QDs, respectively, where insets are the high resolution TEM images.

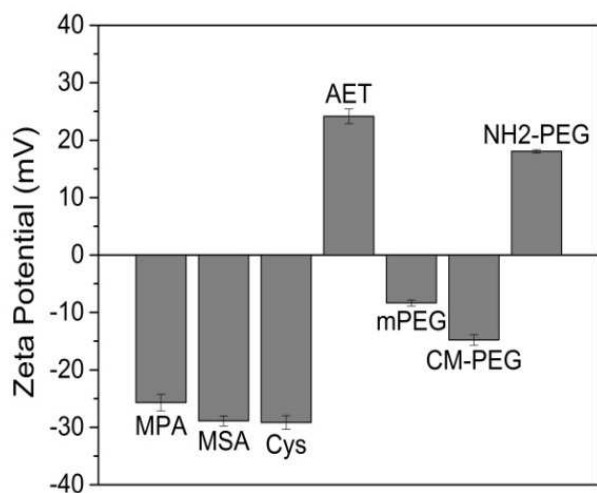


Figure 3. Zeta Potential measurements of QDs ligand exchanged with different surfactants: MPA, MSA, Cys, AET, mPEG, CM-PEG and NH<sub>2</sub>-PEG.

The colloidal stability of the prepared QD formulations in water was monitored by measuring their hydrodynamic size at various time points (see Figure 4). All the prepared formulations here have different colloidal stability and shelf life ranging from period of days to weeks. The MPA- and CM-PEG-capped QDs are the most stable formulations as their hydrodynamic sizes kept almost unchanged over the course of more than 10 days. The MSA- and mPEG-QDs had a slight increase in the hydrodynamic size after aging the samples for one week while Cys- and NH<sub>2</sub>-PEG-QDs showed an obvious size increase due to aggregation of the nanoparticles. The Cys-capped QDs were discovered to be the formulation most prone to aggregation and this is probably due to the coexistence of carboxyl and amino groups on the QDs surface. In general, QDs terminated with carboxyl groups on their surface displayed a much better colloidal stability than those terminated with amino groups on the particle surface. Some reports have demonstrated that the aggregation is attributed to the desorption of the ligands from the QDs surface and this is due to the instability of dynamic nature of thiol-Zn interactions on the QDs surface and the ease of oxidation of the ligands in aqueous dispersions.<sup>31</sup>

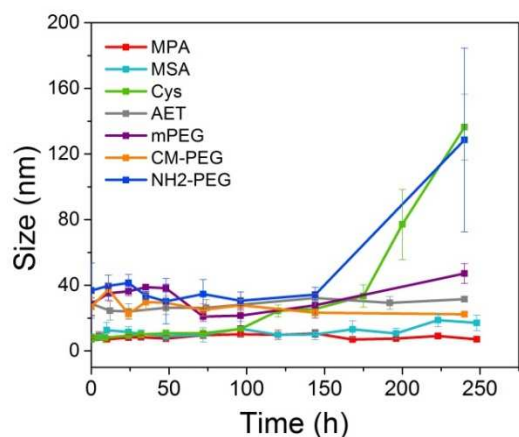


Figure 4. Time dependent hydrodynamic size monitoring of MPA-QDs, Cys-QDs, AET-QDs, mPEG-QDs, CM-PEG-QDs and NH<sub>2</sub>-PEG-QDs in DI water.

To further examine the colloidal stability of QDs, their hydrodynamic sizes in different pH buffer solutions (pH = 4, 7, or 10, at 25°C) were monitored using DLS technique. The colloidal stability of QDs functionalized with short-chain ligands is susceptible to change in different pH environment. Figure 5a shows the relatively stable conditions of MPA-, Cys-, MSA-, and AET-QD formulations under different pH environment. Other formulations that were not included into the plots had very poor colloidal stability and formed large aggregates during the first two to six hours of stability test. The MPA and MSA functionalized QD formulations are relatively stable in alkaline environment due to the ionization of the carboxyl groups. The aggregation and precipitation of other QD formulations might have been resulted from the weakening of Coulombic interactions between particles when they are dispersed in electrolyte solution.<sup>52</sup> The Coulombic interaction of the nanoparticles arises from the repulsive electrostatic force between individual nanoparticles sharing similar surface charge

potentials. On the other hand, the QDs capped with PEG chains were much more colloidal stable in buffer solutions. This is due to the steric stabilization from the long PEG chains and the hydrogen bonding of PEG molecules in water.<sup>23</sup> Figure 5b, c and d suggested that the surface functional groups on the PEG molecules play an important role in determining the colloidal stability life span of the QDs formulation in solutions of varying pH. The CM-PEG-QDs are much more stable in pH 10 buffer solution than in pH 4 solution while a different trend was observed for NH<sub>2</sub>-PEG-QDs formulation. Figure 5d shows that aggregation of particles was observed for NH<sub>2</sub>-PEG-QDs formulation dispersed in both pH 4 and 10 buffer solutions. This is not surprising since the ionization of the carboxyl/amino groups in alkaline/acidic environments might have manipulated particle surface charge whereby enhancing or weakening the electrostatic repulsion forces between particles. Aqueous solution at low pH has numerous hydrogen ions (H<sup>+</sup>) and ease the protonation of amino groups while suppress the dissociation of carboxyl groups. On the other hand, high pH solution is rich in hydroxide ions (OH<sup>-</sup>), which facilitates the dissociation of carboxyl groups but make it difficult for amino groups to acquire hydrogen to be ionized. Interestingly, we have observed that the PEG modified QDs do not favourably interact with water when they are placed in buffer with pH 7. All PEG modified QD formulations started to aggregate in pH 7 buffer solution after 25 to 100 hours. The hydrogen bonds forming between the PEG chains and the water molecules are the main factor that supports the colloidal stability of the QDs in electrolyte solution. However, the presence of various salt ions in the neutral buffer solution may have disrupted the formation of hydrogen bonding and thus leading the PEG-modified QDs to aggregate.<sup>53</sup> For *in vitro* applications, the synthesized QDs are required to be mixed with the cell culture medium for imaging and sensing applications. In the cell culture medium, the solution contains amino acids, salts, glucose and vitamins that are essential for the cells growth and these ingredients play a key role in determining the colloidal stability of QDs.<sup>54</sup>

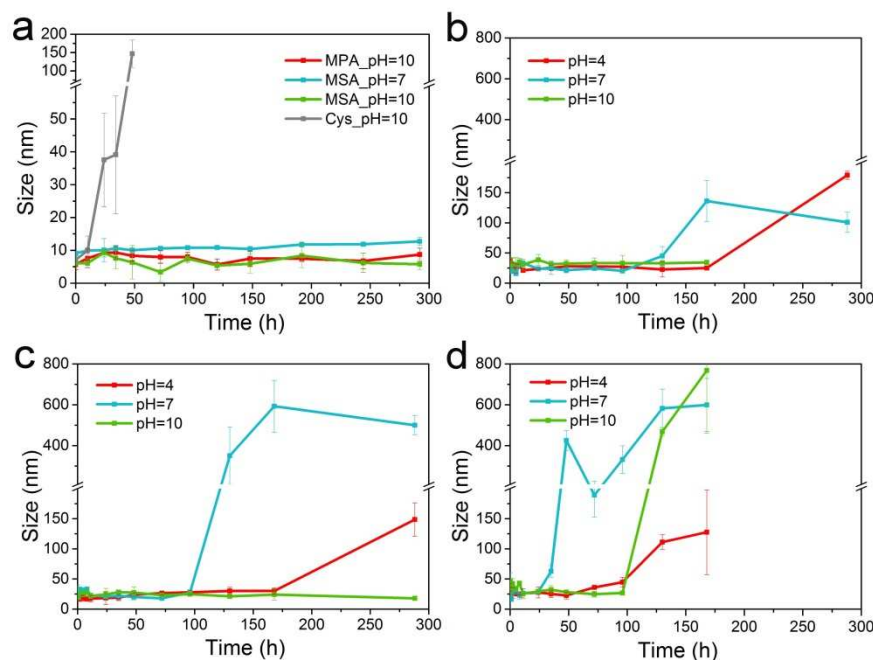


Figure 5. Time dependence of hydrodynamic size of surface modified QDs in pH 4, 7, 10 buffer solutions. QDs were capped with (a) MPA, MSA, Cys, AET (only relatively stable conditions are displayed), (b) mPEG, (c) CM-PEG and (d) NH<sub>2</sub>-PEG.

Figure 6 shows the variation of hydrodynamic diameter of DMEM (Dulbecco's modified Eagle's medium) dispersion of different QD formulations against time. From Figure 6, there is clear surfactant dependence for lengthening the life span of the colloidal stability of DMEM/QDs dispersion. For the short-chain ligand modified QDs, they aggregated in DMEM solution less than a day. The size distribution of the QD aggregates was observed to vary from one hundred to a few hundreds of nanometers. For the case of DMEM dispersion of PEG (mPEG, CM-PEG and NH<sub>2</sub>-PEG) modified QDs, they are relatively more stable than that of short-chain ligands modified QDs since their hydrodynamic diameter size varies less comparing to their initial size. We speculate that this may be due to the PEG modified QDs have better resistance to adsorption of surrounding biomolecules.<sup>55</sup>

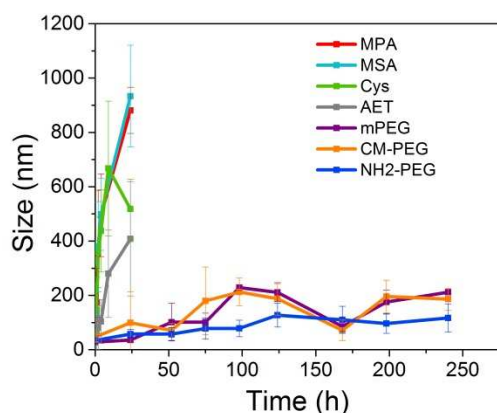


Figure 6. Time dependence of the hydrodynamic size of MPA-QDs, MSA-QDs, Cys-QDs, AET-QDs, mPEG-QDs, CM-PEG-QDs and NH<sub>2</sub>-PEG-QDs in DMEM medium.

Photostability is an important parameter to be considered for selecting the most appropriate fluorescent probes for bioimaging applications. QDs with outstanding photostability are appropriate for applications with long-term excitation and requiring accurate quantitative analysis, such as real-time

molecule tracking and high-resolution 3D reconstruction.<sup>56</sup> Generally, the photostability of QDs are affected by oxygen exposure level,<sup>57</sup> solvents,<sup>58</sup> reducing agents (e.g. mercaptoethanol, dithiothreitol) in solvents,<sup>59</sup> the core compositions and core/shell structure of QDs<sup>60-62</sup> and capping surfactants.<sup>57, 63-65</sup> The evolution of the PL spectra of QDs under irradiation is a common way to examine their photostability. In some cases, UV irradiation may enhance the PL intensity due to photo-induced smoothing and passivation of QD surface.<sup>58</sup> Different mechanisms were proposed to explain the smoothing or passivation process of the QDs surface. For example, most thiol ligands (e.g. MAA, MPA) were reported to passivate the surface defects using adsorbed water molecules, surfactant molecules and new-formed oxide layer.<sup>44</sup> However, the thioglycolic acid (TGA) stabilized QDs formed an additional CdS shell on the surface through the utilization of the sulphur source from TGA ligand.<sup>66</sup> On the other hand, the UV irradiation may also induce corrosion of the QD core<sup>58</sup> and aggregation of QDs,<sup>67</sup> which in turn result in PL degeneration and intensity decrease. In addition, the size of QDs would also change due to photo-corrosion (decrease in size) or coagulation/ripening (increase in size), and consequently causing blue- or red-shift in the PL spectra.<sup>63</sup> In this study, the photoluminescence (PL) spectra of all the prepared QD formulations were monitored under continuous exposure to UV irradiation. Figure 7a shows an example of PL spectra for MPA-QDs formulation after exposing them with UV radiation for different time period and an increase in the PL intensity is observed as radiation exposure time increases. To provide a better understanding on the photostability of the prepared QD formulations, the maximum peak of PL spectra for each formulation was plotted against irradiation time and this is showed in Figure 7b. Except for the AET-QDs formulation, an enhancement in the PL intensity was observed for all the QD formulations in the first few hours of UV irradiation. The variation of PL intensity is due to the photoadsorption and photooxidation reactions occurred on the QDs-thiol interface during the exposure of the QDs formulations to the strong UV irradiation. The photoadsorption reaction will help to remove the surface defects on the QDs surface through an improvement

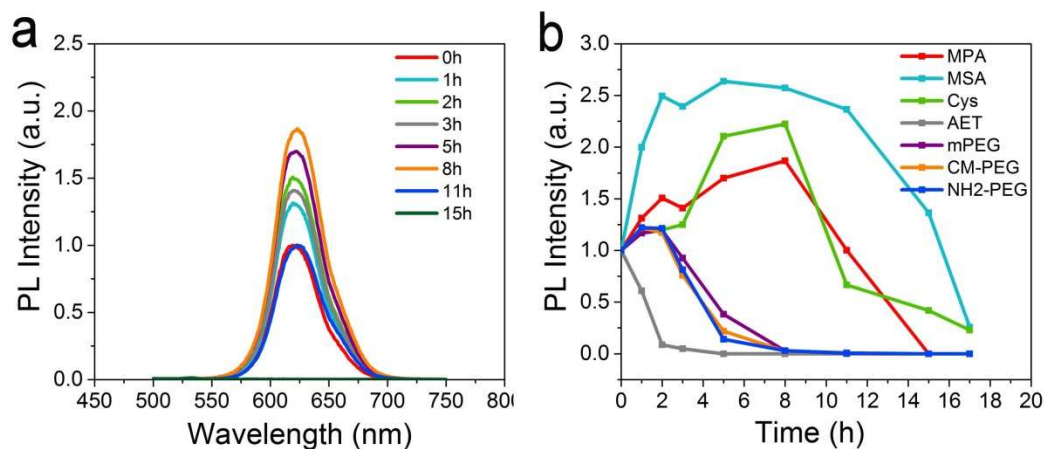


Figure 7. (a) Temporal evolution of the PL spectra of QDs ligand exchanged with MPA. (b) PL maximum changes of MPA-QDs, Cys-QDs, AET-QDs, mPEG-QDs, CM-PEG-QDs and NH<sub>2</sub>-PEG-QDs during different UV irradiation times.



surface passivation process where the coordination of thiols (from ligands) or water molecules with QD surface atoms is enhanced whereby increasing the PL intensity of QDs.<sup>58, 68</sup> In the beginning of the photo-induced oxidation process, a thin oxide layer is formed to passivate the QDs and increase their PL intensity. However, further oxidation leads to the photo-corrosion and aggregation of QDs, of which both are responsible for the PL degeneration.<sup>44, 67</sup> Figure 7b also showed that MPA-, MSA- and Cys-QDs had a longer and larger PL enhancement process than mPEG-, CM-PEG- and NH<sub>2</sub>-PEG-QDs. We speculate that this may arise from the difference in the grafting density of the thiol ligands on QDs. Since the PEG ligands are relatively large, they might have a lower grafting density on QD surface (Supporting Information). As a result, the PEG ligands could be consumed by oxidation more quickly during the PL enhancement process. The unprotected QDs surfaces are prone to be corroded and form surface defects, which causes a faster decrease of the PL intensity. As for the AET-QD formulation, it only showed a relatively quick decrease in the PL intensity. This might result from the instability of AET ligand, which is easily oxidized to its disulphide state at room temperature.<sup>69</sup> Therefore, without the insulation by sufficient AET ligands, the partially naked QDs are liable to form surface defects or aggregate and thus display a quick decrease in their PL intensity.

Nonspecific cell uptake of QDs is a common strategy used to evaluate the feasibility of using the prepared QDs for bioimaging applications. The cellular uptake rate of QDs is greatly affected by several key factors derived from the surface coatings of the QDs, such as the size, surface charge and functional groups.<sup>34, 70-72</sup> It is also cell-type specific and dose dependent.<sup>72, 73</sup> The internalization of nanoparticles by SK-BR-3 cells was observed to be most efficient within 25-50 nm size range.<sup>74</sup> This is a general rule for most nonphagocytic cells whereas phagocytic cells preferentially ingest particles in the range between 2-3  $\mu\text{m}$ .<sup>73</sup> The surface charge affects the cellular uptake but this influence is also cell-type specific. Park et al. have shown that Hela cells have a larger and more rapidly uptake of positively charged QDs than negatively charged QDs while there is almost no internalization for neutral QDs.<sup>75</sup> Similar results were found by Tan et al. for HepG2 and NIH3T3 cells.<sup>72</sup> In contrast to these nonphagocytic cells, most phagocytic cells have stronger interaction with negatively charged particles.<sup>73</sup> To reduce the nonspecific cellular uptake, various strategies were proposed, such as using zwitterionic QDs (e.g. bovine serum albumin (BSA),<sup>76</sup> penicillamine<sup>77</sup>), lysine cross-linked mercapto-acid QDs<sup>35</sup> and hydroxylated QDs.<sup>78</sup> Among these strategies, PEGylation of the QD surface

is the most commonly employed method. The reduction in the cellular uptake was attributed to minimal functional groups from PEG chains<sup>34</sup> and the steric repulsive barrier between PEG-modified QDs and cells.<sup>79-81</sup> Different length and density of PEG chains also account for different cellular uptake rates.<sup>34, 82, 83</sup> It should be noted that nonspecific binding amount of nanoparticles varies for each cell type.<sup>76, 82</sup> In this work, the cell uptake of QDs by RAW246.7 macrophages was carried out for all the synthesized QD formulations. Figure 8 shows the differential interference contrast (DIC) and fluorescent images of RAW246.7 macrophages cells treated with MPA-, Cys-, AET-, mPEG-, CM-PEG- and NH<sub>2</sub>-PEG-QD formulations.

Upon comparing to short-chain ligands modified QDs, minimal uptake of PEG-functionalized QDs was observed in the cells, which is consistent with the previous reports.<sup>34, 72, 84</sup> A strong uptake of MPA- and Cys-QDs was observed after treating the cells with QDs for 4 hours. MSA-QDs formulation was found to exhibit a lower uptake when compared to the MPA- and Cys-QD formulations even though their zeta potential value and hydrodynamic size were almost the same. The preference of QDs uptake may be influenced by the different aggregation state of the nanoparticles. Commonly, most nonphagocytic cells take up cationic nanoparticles to a higher extent than anionic nanoparticles<sup>72</sup> whereas phagocytic cells interact preferentially with anionic nanoparticles.<sup>73</sup> In our case, we observed that anionic charged QD formulations such as MPA-, Cys-, MSA-, mPEG-, CM-PEG-QDs displayed a higher cell uptake by RAW246.7 macrophage cells in comparison to the cationic charged QDs such as AET- and NH<sub>2</sub>-PEG-QDs. Sakai et al. showed that, for PC12 cells, the carboxyl-group modified QDs were taken up more effectively than the amino-group modified QDs.<sup>85</sup> Clift et al. reported that the carboxyl-group modified QDs were rapidly taken up by the J774.A1 macrophage cells based on the endocytic mechanism.<sup>84</sup> Our result is consistent with their observation where similarly we have determined that carboxyl-terminated QDs formulation is having a higher uptake than that of the amino-terminated QDs. In addition, the cellular uptake has been quantified by flow cytometry analysis. The representative plots of the fluorescence intensity in RAW246.7 macrophages treated with or without QD formulations were given in Figure 9. The results are consistent with the patterns obtained from the fluorescent imaging. In general, a relatively high cellular uptake of QDs functionalized with short-chain ligands were observed upon comparing to PEG modified QDs. The strongest fluorescent signals were found in the cells treated with MPA-QDs and Cys-QDs formulation.

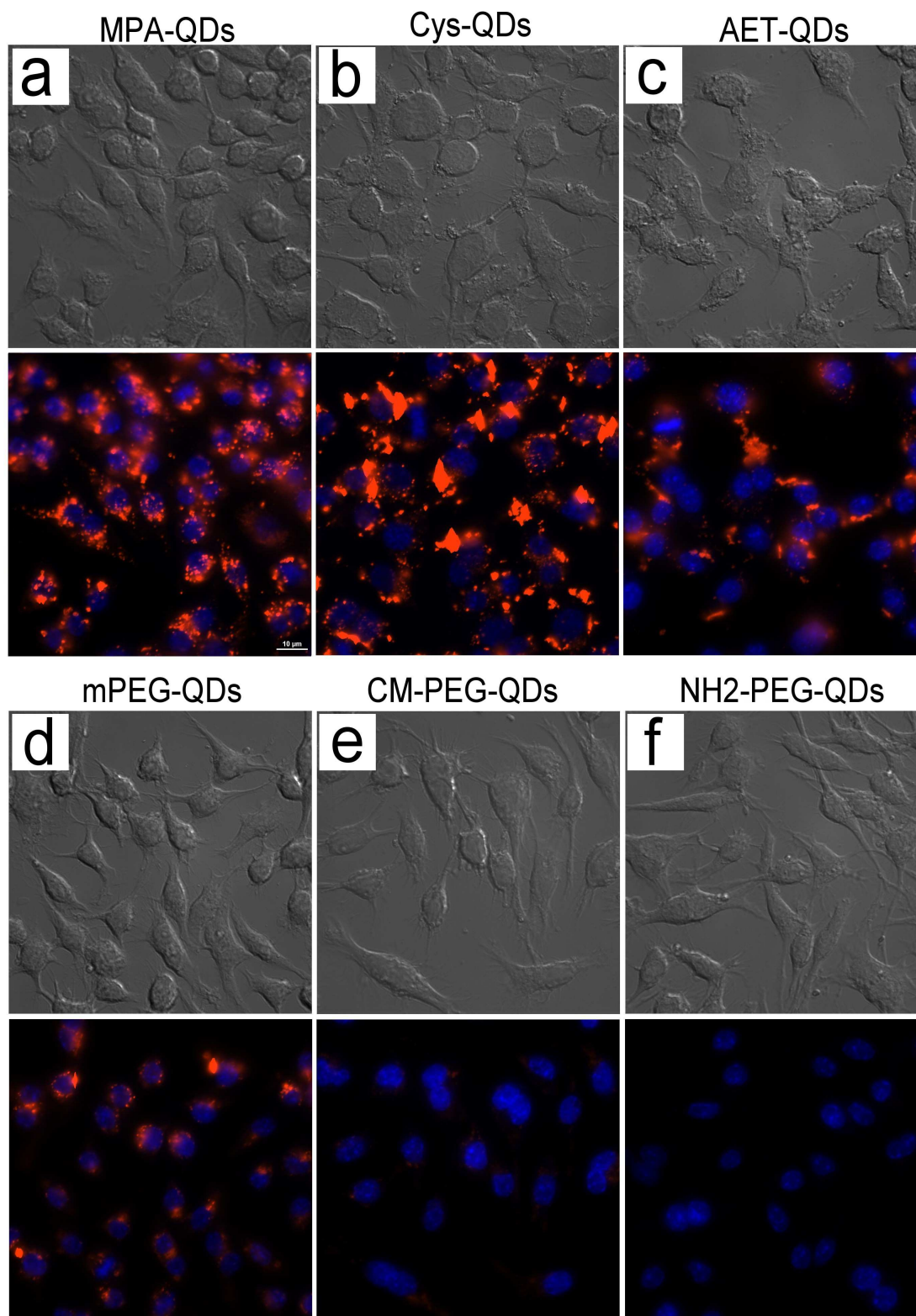


Figure 8. Fluorescent imaging of RAW246.7 cells labeled with different QD formulations through nonspecific uptake. (a) MPA-QDs, (b) Cys-QDs, (c) AET-QDs, (d) mPEG-QDs, (e) CM-PEG-QDs and (f) NH<sub>2</sub>-PEG-QDs. Cell nucleus were stained with DAPI (rendered in blue) and signals from QDs were rendered in red.

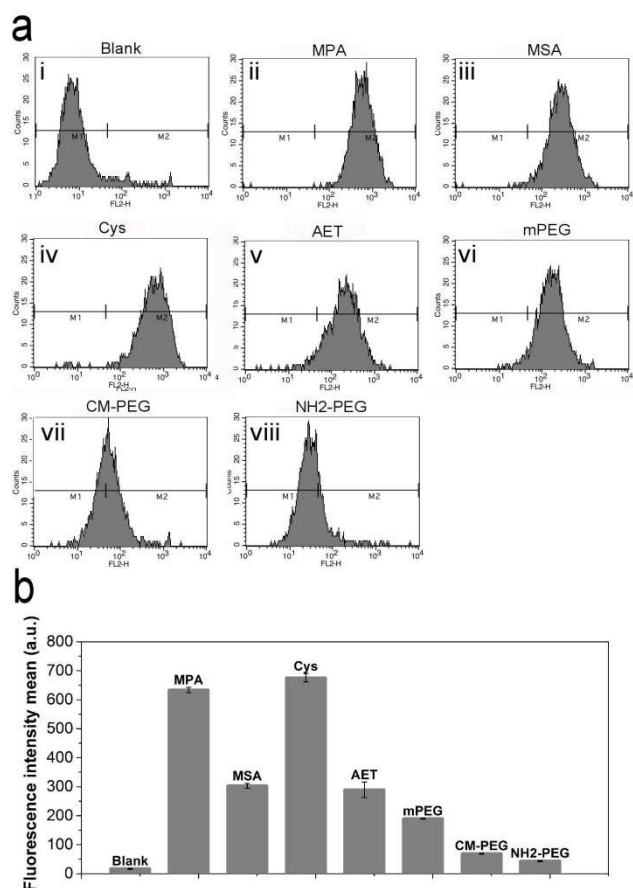


Figure 9. Fluorescence intensity of RAW246.7 macrophage cells determined by flow cytometry analysis. (a) Representative pictures, where cells were treated with (i) PBS, (ii) MPA-QDs, (iii) MSA-QDs, (iv) Cys-QDs, (v) AET-QDs (vi) mPEG-QDs, (vii) CM-PEG-QDs and (viii) NH<sub>2</sub>-PEG-QDs. (b) Average fluorescence intensity from the flow cytometry, n=3.

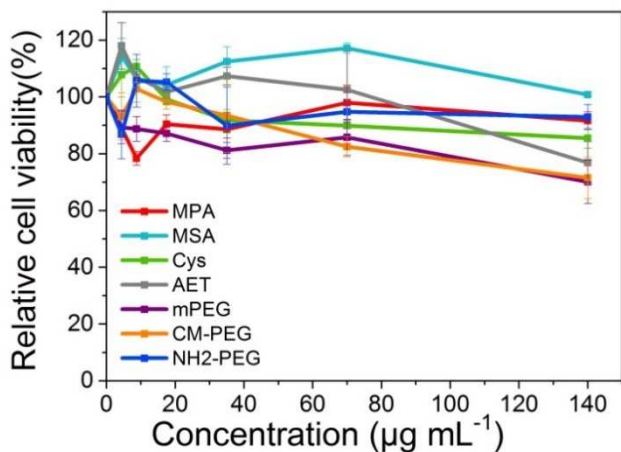


Figure 10. Relative cell viability of RAW246.7 macrophages treated with varying concentrations of MPA-QDs, MSA-QDs, Cys-QDs, AET-QDs, mPEG-QDs, CM-PEG-QDs and NH<sub>2</sub>-PEG-QDs for 24h, n=5.

The toxicity of QDs has been extensively studied for the last decade to understand their impact on the biological systems. Early studies have revealed that the QDs attached with

ligands such as MPA and AET were degraded in the biological environment due to the oxidation of the QDs and this caused the release of heavy metal ions (e.g. Cd<sup>2+</sup>, Pb<sup>2+</sup>) from the particle surface.<sup>86, 87</sup> Applying cross-linked molecules (e.g. BSA<sup>86</sup>) or multidentate polymers on the QDs surface (e.g. DHLA-PEG) may help to minimize the release of the toxic components, whereas using heavy-metal-free QDs (e.g. silicon QDs<sup>88</sup>) will lower the QDs toxicity concern. Recently, Zheng et al. have examined the toxicity of a series of thiol-capped QDs.<sup>89</sup> They have found that the negatively charged glutathione (GSH) coated QDs have the lowest toxicity while the positively charged polyethylenimine (PEI) coated QDs are the most cytotoxic to HaCaT cells among other formulations tested. In addition, incomplete purification<sup>90</sup> of QDs sample may leave some unwashed impurities in the dispersion and induce the toxicological response.<sup>91</sup> Besides from these factors, toxicity could also result from the intrinsic property of QDs, such as their size<sup>92</sup> or reactive oxygen species (ROS) generated on the QDs surface when they are excited by light.<sup>93</sup> It is worth noting that the physiological environment may also change the size, surface charge and agglomeration states of QDs and these changes will have a significant impact on the toxicological responses from the cells.<sup>94</sup> Also, after QDs are introduced into the cell culture system or in the body, proteins will generally be absorbed onto the QD surface and such “complex” may result in changes of the protein activities whereby leading to certain dysfunctions in the biological parts *in vitro* and *in vivo*.<sup>95</sup> All these impacts to the biological systems are directly related to the surface functionalization of the QDs. Thus, continuation and extensive studies are needed to further investigate and understand the underlying mechanisms of QDs toxicity *in vitro* and *in vivo*. In this study, the cytotoxicity of all the QD formulations was evaluated by MTT assays. Figure 10 shows the cell viability of RAW246.7 macrophages cells after treating them with seven QD formulations for 24 hours. The cells treated with the MSA-QD formulation display the highest viability, followed by the NH<sub>2</sub>-PEG- and MPA-QD formulations. All the QD formulations maintained greater than 80% cell viability even at concentrations as high as 120 μg ml<sup>-1</sup>. It is worth mentioning that the concentrations used for cell imaging is much lower than the value of 120 μg ml<sup>-1</sup> used in the MTT assays. This suggests that the prepared QD formulations have negligible toxicity for cell imaging thus could be functionalized with biomolecules and find wide applications for *in vitro* studies. As an example, *in vitro* cellular delivery of fluorescent FAM labeled siRNAs was demonstrated using AET-QDs as carriers. siRNAs are small interfering RNAs with a typical length of 20–25 base pairs. When delivered into the cytoplasm, the sequence-specific siRNAs initiate the RNA interference process and thus regulate the expression of a targeting gene for gene therapy.<sup>96, 97</sup> However, free siRNAs are fragile and negatively charged. They are liable to degradation in biological fluids or could not penetrate the cell membrane by themselves without a proper carrier.<sup>98, 99</sup> In this example, siRNAs were conjugated with the positively charged AET-QDs through electrostatic interaction (Supplementary information, Figure S2) and were successfully delivered into cell cytoplasm (Supplementary information, Figure S3).

## Conclusions

In summary, we have performed a detailed study in understanding the effects of surface ligands on the physical property, optical and colloidal stability, cellular uptake and *in vitro* cytotoxicity of QDs. Our result indicates that PEG

modified QDs have a higher colloidal stability and they have lower uptake in the cells upon comparing to short-chain ligand modified QD formulations. However, PEG modified QDs displayed a relatively large hydrodynamic diameter size and they have poor photostability. For carboxyl-terminated QD formulations, these formulations possess an excellent colloidal stability in water and alkaline buffer solutions. MSA-QDs were revealed to be most stable in neutral and alkaline buffer solutions and also possess best photostability. Our study suggested that the preference of QDs cell uptake is strongly correlated with the surface charge density of QDs. We have found that the anionic QDs were having much higher cell uptake in comparison to the cationic QD formulations for RAW246.7 macrophage cells. Overall, the physicochemical property of QDs is sensitively influenced by the type of surface ligands used to modify the QDs surface. Thus, it is important to consider the length, surface charge, grafting density and functional groups of the surface ligands in designing the desirable QDs formulation for specific biological applications. It is worth noting that there are diverse QD ligands exchange protocols available in the literature and slight changes in the preparation parameters will result in different quality of QD aqueous dispersion. As such, it is imperative to follow the same set of protocol when preparing the QDs dispersion with specific type of surface ligands. In general, each set of prepared QD formulation with specific type of surface ligands will display some limitations in certain aspects of their physicochemical property and therefore we should carefully consider and choose the type of QDs required to be used in the experiments thereby minimizing their impacts arising from their limitation factors.

### Acknowledgements

The study was supported by the Start-up grant (M4080141.040) from Nanyang Technological University, Tier1 Academic Research Funds (M4010360.040 RG29/10) from Singapore Ministry of Education and partially from the Singapore Ministry of Education under Tier 2 Research Grant MOE2010-T2-2-010 (4020020.040 ARC2/11).

### Notes and references

<sup>a</sup>School of Electrical and Electronic Engineering, Nanyang Technological University, Singapore 639798, Singapore

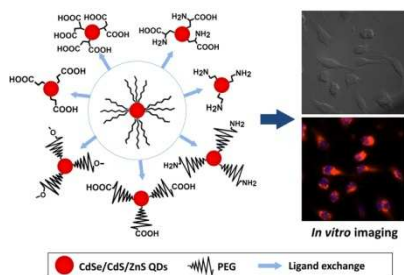
<sup>b</sup>Department of Chemical and Biological Engineering, University at Buffalo (SUNY), Buffalo, New York 14260, United States

\*Corresponding author: Ken-Tye Yong, PhD, School of Electrical and Electronic Engineering, Nanyang Technological University, Singapore 639798, Singapore Tel: +65-6790-5444, email: [kt Yong@ntu.edu.sg](mailto:kt Yong@ntu.edu.sg)

† Electronic Supplementary Information (ESI) available: [details of any supplementary information available should be included here]. See DOI: 10.1039/b000000x/

1. F. Pinaud, S. Clarke, A. Sittner and M. Dahan, *Nature Methods*, 2010, **7**, 275-285.
2. A. M. Smith, H. W. Duan, A. M. Mohs and S. M. Nie, *Advanced Drug Delivery Reviews*, 2008, **60**, 1226-1240.
3. I. L. Medintz, H. T. Uyeda, E. R. Goldman and H. Mattoussi, *Nature Materials*, 2005, **4**, 435-446.
4. X. Michalet, F. F. Pinaud, L. A. Bentolila, J. M. Tsay, S. Doose, J. J. Li, G. Sundaresan, A. M. Wu, S. S. Gambhir and S. Weiss, *Science*, 2005, **307**, 538-544.
5. M. Bruchez, M. Moronne, P. Gin, S. Weiss and A. P. Alivisatos, *Science*, 1998, **281**, 2013-2016.
6. T. L. Doane and C. Burda, *Chemical Society Reviews*, 2012, **41**, 2885-2911.
7. Y. C. Wang, R. Hu, G. M. Lin, I. Roy and K. T. Yong, *ACS Applied Materials & Interfaces*, 2013, **5**, 2786-2799.
8. U. Resch-Genger, M. Grabolle, S. Cavaliere-Jaricot, R. Nitschke and T. Nann, *Nature Methods*, 2008, **5**, 763-775.
9. S. Jiang, K. Y. Win, S. H. Liu, C. P. Teng, Y. G. Zheng and M. Y. Han, *Nanoscale*, 2013, **5**, 3127-3148.
10. A. R. Clapp, I. L. Medintz and H. Mattoussi, *Chemphyschem*, 2006, **7**, 47-57.
11. W. C. W. Chan, D. J. Maxwell, X. H. Gao, R. E. Bailey, M. Y. Han and S. M. Nie, *Current Opinion in Biotechnology*, 2002, **13**, 40-46.
12. R. J. Byers and E. R. Hitchman, *Progress in Histochemistry and Cytochemistry*, 2011, **45**, 201-237.
13. M. V. Yezhelyev, L. F. Qi, R. M. O'Regan, S. Nie and X. H. Gao, *Journal of the American Chemical Society*, 2008, **130**, 9006-9012.
14. C. J. Xu, L. Y. Mu, I. Roes, D. Miranda-Nieves, M. Nahrendorf, J. A. Ankrum, W. A. Zhao and J. M. Karp, *Nanotechnology*, 2011, **22**.
15. V. Biju, S. Mundayoor, R. V. Omkumar, A. Anas and M. Ishikawa, *Biotechnology Advances*, 2010, **28**, 199-213.
16. L. F. Qi and X. H. Gao, *Expert Opinion on Drug Delivery*, 2008, **5**, 263-267.
17. J. A. Kloepfer, R. E. Mielke and J. L. Nadeau, in *Quantum Dots, Nanoparticles, and Nanoclusters*, eds. D. L. Huffaker and P. Bhattacharya, 2004, vol. 5361, pp. 133-141.
18. B. K. Pong, B. L. Trout and J. Y. Lee, *Langmuir*, 2008, **24**, 5270-5276.
19. V. Biju, T. Itoh and M. Ishikawa, *Chemical Society Reviews*, 2010, **39**, 3031-3056.
20. V. Biju, T. Itoh, A. Anas, A. Sujith and M. Ishikawa, *Analytical and Bioanalytical Chemistry*, 2008, **391**, 2469-2495.
21. R. A. Sperling and W. J. Parak, *Philosophical Transactions of the Royal Society a-Mathematical Physical and Engineering Sciences*, 2010, **368**, 1333-1383.
22. N. Erathodiyil and J. Y. Ying, *Accounts of Chemical Research*, 2011, **44**, 925-935.
23. F. Zhang, E. Lees, F. Amin, P. R. Gil, F. Yang, P. Mulvaney and W. J. Parak, *Small*, 2011, **7**, 3113-3127.
24. J. H. Lee, K. Lee, S. H. Moon, Y. Lee, T. G. Park and J. Cheon, *Angewandte Chemie-International Edition*, 2009, **48**, 4174-4179.
25. R. Hu, Y. C. Wang, X. Liu, G. M. Lin, C. H. Tan, W. C. Law, I. Roy and K. T. Yong, *RSC Advances*, 2013, **3**, 8495-8503.
26. N. Tomczak, D. Janczewski, M. Y. Han and G. J. Vancso, *Progress in Polymer Science*, 2009, **34**, 393-430.
27. Y. Zhang, M. Wang, Y. G. Zheng, H. Tan, B. Y. W. Hsu, Z. C. Yang, S. Y. Wong, A. Y. C. Chang, M. Choolani, X. Li and J. Wang, *Chemistry of Materials*, 2013, **25**, 2976-2985.
28. J. T. Song, S. J. Wu and Y. L. Zhao, *Materials Research Bulletin*, 2013, **48**, 1530-1535.
29. W. Liu, M. Howarth, A. B. Greytak, Y. Zheng, D. G. Nocera, A. Y. Ting and M. G. Bawendi, *Journal of the American Chemical Society*, 2008, **130**, 1274-1284.
30. S. B. Brichkin and E. V. Chernykh, *High Energy Chemistry*, 2011, **45**, 1-12.
31. W. H. Liu, H. S. Choi, J. P. Zimmer, E. Tanaka, J. V. Frangioni and M. Bawendi, *Journal of the American Chemical Society*, 2007, **129**, 14530-+.
32. S. F. Wuister, I. Swart, F. van Driel, S. G. Hickey and C. D. Donega, *Nano Letters*, 2003, **3**, 503-507.
33. A. M. Smith and S. Nie, *Journal of the American Chemical Society*, 2008, **130**, 11278-+.
34. T. A. Kelf, V. K. A. Sreenivasan, J. Sun, E. J. Kim, E. M. Goldys and A. V. Zvyagin, *Nanotechnology*, 2010, **21**.
35. W. Jiang, S. Mardiyani, H. Fischer and W. C. W. Chan, *Chemistry of Materials*, 2006, **18**, 872-878.
36. A. Hoshino, K. Fujioka, T. Oku, M. Suga, Y. F. Sasaki, T. Ohta, M. Yasuhara, K. Suzuki and K. Yamamoto, *Nano Letters*, 2004, **4**, 2163-2169.
37. L. Ye, K. T. Yong, L. W. Liu, I. Roy, R. Hu, J. Zhu, H. X. Cai, W. C. Law, J. W. Liu, K. Wang, J. Liu, Y. Q. Liu, Y. Z. Hu, X. H. Zhang, M. T. Swihart and P. N. Prasad, *Nature Nanotechnology*, 2012, **7**, 453-458.

38. M. Taibi, S. Ammar, N. Jouini, F. Fievet, P. Molinie and M. Drillon, *Journal of Materials Chemistry*, 2002, **12**, 3238-3244.
39. J. W. Lee, W. C. Choi and J. D. Kim, *Crystengcomm*, 2010, **12**, 3249-3254.
40. S. S. L. Sobhana, M. V. Devi, T. P. Sastry and A. B. Mandal, *Journal of Nanoparticle Research*, 2011, **13**, 1747-1757.
41. T. Y. Dong, W. T. Chen, C. W. Wang, C. P. Chen, C. N. Chen, M. C. Lin, J. M. Song, I. G. Chen and T. H. Kao, *Physical Chemistry Chemical Physics*, 2009, **11**, 6269-6275.
42. H. B. Li, C. P. Han and L. Zhang, *Journal of Materials Chemistry*, 2008, **18**, 4543-4548.
43. R. C. Advincula, *Dalton Transactions*, 2006, 2778-2784.
44. C. Barrera, A. P. Herrera and C. Rinaldi, *Journal of Colloid and Interface Science*, 2009, **329**, 107-113.
45. C. Y. Wang, L. L. Feng, H. Z. Yang, G. B. Xin, W. Li, J. Zheng, W. H. Tian and X. G. Li, *Physical Chemistry Chemical Physics*, 2012, **14**, 13233-13238.
46. J. E. B. Katari, V. L. Colvin and A. P. Alivisatos, *Journal of Physical Chemistry*, 1994, **98**, 4109-4117.
47. C. Bullen and P. Mulvaney, *Langmuir*, 2006, **22**, 3007-3013.
48. G. Sui, J. Orbulescu, X. J. Ji, K. M. Gattas-Asfura, R. M. Leblanc and M. Micic, *Journal of Cluster Science*, 2003, **14**, 123-133.
49. W. P. Wuelfing, S. M. Gross, D. T. Miles and R. W. Murray, *Journal of the American Chemical Society*, 1998, **120**, 12696-12697.
50. X. L. Huang, L. M. Bronstein, J. Retrum, C. Dufort, I. Tsvetkova, S. Anagyeyi, B. Stein, G. Stucky, B. McKenna, N. Remmes, D. Baxter, C. C. Kao and B. Dragnea, *Nano Letters*, 2007, **7**, 2407-2416.
51. M. Kuno, J. K. Lee, B. O. Dabbousi, F. V. Mikulec and M. G. Bawendi, *Journal of Chemical Physics*, 1997, **106**, 9869-9882.
52. W. J. Parak, D. Gerion, T. Pellegrino, D. Zanchet, C. Micheel, S. C. Williams, R. Boudreau, M. A. Le Gros, C. A. Larabell and A. P. Alivisatos, *Nanotechnology*, 2003, **14**, R15-R27.
53. V. V. Khutoryanskiy, G. A. Mun, Z. S. Nurkeeva and A. V. Dubolazov, *Polymer International*, 2004, **53**, 1382-1387.
54. I. Ojeda-Jimenez, J. Piella, T. L. Nguyen, A. Bestetti, A. D. Ryan, V. Puentes and Iop, in *Nanosafe 2012: International Conferences on Safe Production and Use of Nanomaterials*, 2013, vol. 429.
55. A. J. Wang, J. J. Xu and H. Y. Chen, *Journal of Chromatography A*, 2007, **1147**, 120-126.
56. P. Zrazhevskiy, M. Sena and X. H. Gao, *Chemical Society Reviews*, 2010, **39**, 4326-4354.
57. S. Emin, A. Loukanov, M. Wakasa, S. Nakabayashi and Y. Kaneko, *Chemistry Letters*, 2010, **39**, 654-656.
58. C. Carrillo-Carrion, S. Cardenas, B. M. Simonet and M. Valcarcel, *Chemical Communications*, 2009, 5214-5226.
59. E. A. Christensen, P. Kulatunga and B. C. Lagerholm, *Plos One*, 2012, **7**.
60. Y. He, H. T. Lu, L. M. Sai, Y. Y. Su, M. Hu, C. H. Fan, W. Huang and L. H. Wang, *Advanced Materials*, 2008, **20**, 3416-+.
61. F. Aldeek, C. Mustin, L. Balan, G. Medjahdi, T. Roques-Carmes, P. Arnoux and R. Schneider, *European Journal of Inorganic Chemistry*, 2011, 794-801.
62. W.-S. Chae, T. D. T. Ung and Q. L. Nguyen, *Advances in Natural Sciences: Nanoscience and Nanotechnology*, 2013, **4**, 045009.
63. A. M. A. Morshed and T. H. Yoon, *Bulletin of the Korean Chemical Society*, 2008, **29**, 249-251.
64. D. L. Nida, N. Nitin, W. W. Yu, V. L. Colvin and R. Richards-Kortum, *Nanotechnology*, 2008, **19**.
65. Isnaeni, L. H. Jin and Y. H. Cho, *Journal of Colloid and Interface Science*, 2013, **395**, 45-49.
66. H. Peng, L. J. Zhang, C. Soeller and J. Travas-Sejdic, *Journal of Luminescence*, 2007, **127**, 721-726.
67. J. Aldana, Y. A. Wang and X. G. Peng, *Journal of the American Chemical Society*, 2001, **123**, 8844-8850.
68. Z. Zhelev, R. Jose, T. Nagase, H. Ohba, R. Bakalova, M. Ishikawa and Y. Baba, *Journal of Photochemistry and Photobiology B-Biology*, 2004, **75**, 99-105.
69. F. Iwata, E. M. Kuehl, G. F. Reed, L. M. McCain, W. A. Gahl and M. I. Kaiser-Kupfer, *Molecular Genetics and Metabolism*, 1998, **64**, 237-242.
70. L. W. Zhang and N. A. Monteiro-Riviere, *Toxicological Sciences*, 2009, **110**, 138-155.
71. Y. Choi, K. Kim, S. Hong, H. Kim, Y. J. Kwon and R. Song, *Bioconjugate Chemistry*, 2011, **22**, 1576-1586.
72. S. J. Tan, N. R. Jana, S. J. Gao, P. K. Patra and J. Y. Ying, *Chemistry of Materials*, 2010, **22**, 2239-2247.
73. E. Frohlich, *International Journal of Nanomedicine*, 2012, **7**, 5577-5591.
74. W. Jiang, B. Y. S. Kim, J. T. Rutka and W. C. W. Chan, *Nature Nanotechnology*, 2008, **3**, 145-150.
75. J. Park, J. Nam, N. Won, H. Jin, S. Jung, S. H. Cho and S. Kim, *Advanced Functional Materials*, 2011, **21**, 1558-1566.
76. B. B. Zhang, X. H. Wang, F. J. Liu, Y. S. Cheng and D. L. Shi, *Langmuir*, 2012, **28**, 16605-16613.
77. V. V. Breus, C. D. Heyes, K. Tron and G. U. Nienhaus, *Acs Nano*, 2009, **3**, 2573-2580.
78. B. A. Kairdolf, M. C. Mancini, A. M. Smith and S. M. Nie, *Analytical Chemistry*, 2008, **80**, 3029-3034.
79. M. A. Dobrovolskaia, P. Aggarwal, J. B. Hall and S. E. McNeil, *Molecular Pharmaceutics*, 2008, **5**, 487-495.
80. V. Stone, H. Johnston and M. J. D. Clift, *Ieee Transactions on Nanobioscience*, 2007, **6**, 331-340.
81. M. J. D. Clift and V. Stone, *Theranostics*, 2012, **2**, 668-680.
82. E. L. Bentzen, I. D. Tomlinson, J. Mason, P. Gresch, M. R. Warnement, D. Wright, E. Sanders-Bush, R. Blakely and S. J. Rosenthal, *Bioconjugate Chemistry*, 2005, **16**, 1488-1494.
83. C. D. Walkey, J. B. Olsen, H. B. Guo, A. Emili and W. C. W. Chan, *Journal of the American Chemical Society*, 2012, **134**, 2139-2147.
84. M. J. D. Clift, B. Rothen-Rutishauser, D. M. Brown, R. Duffin, K. Donaldson, L. Proudfoot, K. Guy and V. Stone, *Toxicology and Applied Pharmacology*, 2008, **232**, 418-427.
85. N. Sakai, Y. Matsui, A. Nakayama, A. Tsuda and M. Yoneda, *Journal of Physics: Conference Series*, 2011, **304**, 012049.
86. A. M. Derfus, W. C. W. Chan and S. N. Bhatia, *Nano Letters*, 2004, **4**, 11-18.
87. C. Kirchner, T. Liedl, S. Kuder, T. Pellegrino, A. M. Javier, H. E. Gaub, S. Stolze, N. Fertig and W. J. Parak, *Nano Letters*, 2005, **5**, 331-338.
88. J. Y. Fan and P. K. Chu, *Small*, 2010, **6**, 2080-2098.
89. H. Zheng, L. J. Mortensen and L. A. DeLouise, *Journal of Biomedical Nanotechnology*, 2013, **9**, 382-392.
90. Y. Shen, M. Y. Gee, R. Tan, P. J. Pellechia and A. B. Greytak, *Chemistry of Materials*, 2013, **25**, 2838-2848.
91. C. Park, D. H. Kim, M. J. Kim and T. H. Yoon, *Bulletin of the Korean Chemical Society*, 2008, **29**, 303-304.
92. A. Shiohara, A. Hoshino, K. Hanaki, K. Suzuki and K. Yamamoto, *Microbiology and Immunology*, 2004, **48**, 669-675.
93. W. W. Yu, E. Chang, R. Drezek and V. L. Colvin, *Biochemical and Biophysical Research Communications*, 2006, **348**, 781-786.
94. J. K. Jiang, G. Oberdorster and P. Biswas, *Journal of Nanoparticle Research*, 2009, **11**, 77-89.
95. B. Pelaz, G. Charron, C. Pfeiffer, Y. L. Zhao, J. M. de la Fuente, X. J. Liang, W. J. Parak and P. del Pino, *Small*, 2013, **9**, 1573-1584.
96. A. L. Jackson, S. R. Bartz, J. Schelter, S. V. Kobayashi, J. Burchard, M. Mao, B. Li, G. Cavet and P. S. Linsley, *Nature Biotechnology*, 2003, **21**, 635-637.
97. T. R. Brummelkamp, R. Bernards and R. Agami, *Science*, 2002, **296**, 550-553.
98. L. F. Qi, W. J. Shao and D. L. Shi, *Journal of Materials Chemistry B*, 2013, **1**, 654-660.
99. J. M. Li, M. X. Zhao, H. Su, Y. Y. Wang, C. P. Tan, L. N. Ji and Z. W. Mao, *Biomaterials*, 2011, **32**, 7978-7987.



Aqueous CdSe/CdS/ZnS quantum dots with different surface ligands were prepared through ligand exchange and extensively characterized for biological applications.